


Research Article

Experimental Investigations on Single-Phase Heat Transfer Enhancement in an Air-To-Water Heat Exchanger with Rectangular Perforated Flow Deflector Baffle Plate

^{1*}Md A. Rahman 

¹ Department of Mechanical Engineering, Birla Institute of Technology, Mesra, Ranchi, India
E-mail: ^{1*}rahman.md4u@gmail.com

Received 18 April 2023, Revised 13 August 2023, Accepted 28 August 2023

Abstract

Experimental analysis was conducted to investigate the turbulent heat transfer behaviors within a tubular heat exchanger, incorporating a novel baffle plate design. The new design includes a perforated circular baffle plate with a rectangular flow deflector that can be adjusted to different inclination angles. The baffle plate is strategically positioned at the entrance of the heat exchanger, resulting in a swirling flow downstream. To assess the impact of the baffle plate design, three baffle plates were placed longitudinally along the flow, with varying pitch ratios (l/D). The effects of pitch ratio (ranging from 0.6 to 1.2), deflector inclination angle (ranging between 30° to 50°), and Reynolds numbers (ranging between 16000 to 29000) were examined. The outcomes highlighted the substantial impact of pitch ratio and inclination angle on the thermal enhancement factor. In particular, compared to single segmental baffle plates working under similar operating conditions. The result indicates that an inclination angle of 30° and a pitch ratio of 1 exhibited an average 41.49% augmentation in thermal-fluidic performance compared with an exchanger with a segmental baffle plate.

Keywords: Thermal enhancement factor; flow resistance; inclination angle; swirl flow, re-circulation; rectangular deflector.

1. Introduction

Recent population boom and urbanization have led researchers to focus on efficient energy consumption and utilization. To reduce energy consumption, efficient and compact thermal system designs are adopted. HX (heat exchangers) are standard thermal exchange devices widely used in commercials, industrial and domestic sectors. Some typical applications are cooling in power plants, automobiles, domestic, solar dryers, boilers/steam generators, the chemical processing industry, and waste heat recovery. Thus the demand for energy-efficient HX has led to the development of various heat augmentation techniques [1]. Different strategies of heat transfer enhancement, namely active, passive, and compound methods, are suggested [2, 3] with the mutual objective of plummeting thermal boundary layer thickness to achieve an improved surface heat transfer coefficient.

No outside source of heat transfer is needed for the passive approach. This approach involves altering or extending the surfaces to generate turbulence in the flow field. This turbulence can modify the thermal boundary layer and change the flow pattern. Artificial roughness is the most basic turbulence promoter in this form of passive enhancement. Other turbulence promoters associated with this approach include extended surfaces, swirl devices, and vortex generators.

The presence of artificial roughness breaks up the laminar layer located near the wall and causes turbulence to

form between the ridges. This turbulence is created when the flow separates and attaches itself to the wall again, leaving the main flow pattern unaffected. Geometric constraints of surface roughness like channel aspect ratio (AR), rib angle of attack (α), relative rib pitch (p/e), relative rib height ratio (e/D) along with the rib shape and type (solid, perforated, and slit rib, etc.) have a direct influence on heat transfer coefficients. Prasad and Saini [4, 5] studied transverse ribs on the absorber plate of a solar air heater duct. A maximum increment of 2.38 in the relative Nu and a 4.25 increment in relative f when contrasted to smooth duct, with a relative roughness pitch (p/e) of 10 and relative roughness (e/D) of 0.033. Similar work carried out by Prasad et al. [6]. Lu and Jiang [7] investigated the influence of ribs with an inclination angle of 20° and 60° on the thermo-hydraulic performance and heat transfer rate. The research results revealed that the maximum performance and heat transfer rate was achieved at these two angles. Liu et al. [8] experimented to study the consequence of different constraints on a rectangular channel with opposite walls having grooves of different relative pitch (p/e), aspect ratio (W/H), angle of attack (α), and blockage ratio (e/D). The parameters used for the experiment ranged from 0.25 to 1 for p/e , 45 to 60 degrees for angle of attack, and 0.047 to 0.078 for blockage ratio. An attack angle of 45 degrees shows Nu rise by 15-25%.

Another effective technique is to increase the effective heat transfer area and add turbulence to the flow. This method includes extended surfaces as fin/baffles, negatively

impacting pressure drop and requiring higher pumping power. Experimental examination on heat transfer and friction loss by Sriromreum et al. [9] on a zigzag Z-baffle (45°) with relative height and relative pitch range of baffles were of 0.1–0.3 and 1.5–3, respectively. Nu and f were improved significantly for in-phase 45° Z-baffles rather than its counterpart (out-phase 45°). Kwankaomeng et al. [10] numerically studied angled inclined baffles with an attack angle of 30° under a laminar flow regime. The BR and PR variations of (0.1–0.5) and (1–2) revealed an enhancement in Nu and f of 9.23 and 45.31, respectively, for PR of 1.5 and BR of 0.3.

Priyam et al. [11]. Studied the effect of fin pitch and mass flow rate of transverse wavy fins. The results showed an enhancement in thermal efficiency of 62.53, and an effective temperature rise of 63.41%, respectively. Gawande et al. [12] experimental and numerical investigation on an absorber plate with L-shape ribs, with relative roughness, pitch relative rib height range of 7.14–17.86. Results indicated maximum enhancement in Nu and f of 2.827 and 3.424 at a relative pitch of 7.14.

A more recent and promising heat transfer enhancement technique is swirl flow devices. The technique augments heat transfer by applying a twisted tape in the flow stream that can generate swirls by trimming the boundary layer by generating a secondary flow in vortices along an existing axial flow. Recently various swirl devices have been tested, such as conical rings, helical wire, and twisted tapes.

Ard et al. [13] evaluated the effects of wing position (h/e) of square-wing perforated slanting baffles on the heat transfer rate and Δp characteristics in a rectangular channel with air as working fluid drawn in using 3 HP blower and base plate ($L \times W$) heated using 1.0 KW heater. The baffle pitch ratio (p/e) was constant at 5.0, with testing done at different Re values 6000, 9000, 12,000, 15,000, 18,000, 21,000, and 24,000 with four different wings location (h/e) 0.92, 0.83, 0.75, and 0.67. Results showed that the highest heat transfer rates accomplished in channels at the four locations were 148%, 157%, 166%, and 180% compared to smooth channels, while the pressure losses increased 9.51–10.99 times, respectively. Additionally, SW-PBs caused lower Δp than solid transverse baffles and higher thermal performance.

Sanchouli et al. [14] explored the prospective to enhance the heat transfer capabilities of phase change material (PCM) in an HX with a double-tube design by incorporating innovative ring-shaped fins with a lattice structure. These lattice ring-shaped fins, which consisted of straight and circular strip modules, were located on the inner tube. To compare the thermal efficiency of the lattice ring-shaped fins with traditional ring-shaped fins, they ensured that an equal amount of fins was used for the comparison. They also examined how the spacing between the fins (longitudinal pitch) affected the duration of the melting process and the PCM's energy storage capacity. They compared the findings between the lattice and conventional ring-shaped fins.

The domino effect showed that converting the ring-shaped fins to lattice fins reduced the melting time by 27%, 37.5%, 53.5%, and 69.5% for longitudinal pitches of 125 mm, 62.5 mm, 31.25 mm, and 15.625 mm, respectively. Among the different longitudinal pitches, the lattice fins with a spacing of 31.25 mm exhibited the highest thermal performance. The study also emphasized the significance of the arrangement of the lattice ring-shaped fin components in achieving optimal thermal performance. The total melting

time of the PCM was improved by 40% compared to the case with a longitudinal pitch of 125 mm, demonstrating the advantages of the 31.25 mm spacing. The study also considered a non-uniform distribution of lattice components for the ring-shaped fins and observed a 16% enhancement in the full melting time matched to the best ring-shaped fins with a uniform lattice distribution.

Rahman and Dhiman [15, 16] examined the effect of a novel trapezoidal perforated baffle plate on PEC used in air-water HX. The baffle plate was equipped with a trapezoidal flow deflector with its larger end attached to the baffle plate at different α . The effect of PR, α , and flow orientation (parallel and counter flow) on the TEF was studied. The result showed that the TEF is a noteworthy function of PR and α . Specifically, in the range of Re from 16000 to 28000, the duct with perforated flow deflector baffle plates achieved an average of 3.75 times higher performance with a deflector with α of 50° and PR of 1.4. Additionally, when the flow orientation changed from parallel to counter flow, there was an average 7.4% improvement in PEC when the deflector with α was set to 30° , with the highest HX effectiveness observed at lower α and high PR values.

Alam et al. [17] experimentally studied twisted tape inserts of various twist and pitch ratios as heat transfer enhancement devices. The result was an 18–70% increase in heat transfer rate and an 87–132% increase in pressure drop with Re range of 4000 to 10000. Guo et al. [18] numerically investigated the center-cleared twisted tape for heat transfer enhancement, showing an improvement of 7–20% in thermal performance compared to conventional twisted tape

Thianpong et al. [19] studied the combined effect of twisted tape inserted inside a dimpled tube under a turbulent flow regime. Three different twist ratios (3, 5, and 7) and PR (0.7–1) were tested. The result showed that the combined effect of twisted tape and dimples is more prominent on heat transfer and friction factor than dimple or plain tube acting alone. Esmaeilzadeh et al. [20] experimental investigation of heat transfer and pressure drop in a circular tube equipped with a twisted tape of varying thicknesses (0.5–2 mm) revealed that thick tapes are more effective. Bhuiya et al. [21] investigated double counter twisted tapes with varying twist ratios (1.95 to 7.75). A maximum of 240% increase in the heat transfer rate and a 286% increase in friction factor were reported.

The above literature examined various turbulator designs to enhance heat transfer. Emphasis was placed on devices that create swirls to manipulate the flow path, resulting in increased fluid mixing and turbulence. This ultimately leads to enhanced heat transfer within the flow regime. Further, it can also be concluded that turbulators with lower α and baffles with lower PR and lower perforation ratio show the highest Nu compared to smooth duct flow with a parallel rise in Δp . The swirl flow brings along a toroidal recirculation zone. It generates secondary flow, and additional vortices formation, which constantly washes the heat transfer surface area, reducing the thermal boundary layer and increasing hm .

A novel swirler is fabricated and tested in this current hooping for a better TEF index. The swirler is a flat circular perforated baffle plate with a rectangular flow deflector. The flow deflector is attached at different α (angle made by deflector with baffle plate surface). The baffle plate is placed at the entry of the test section to produce a decaying swirl flow, which increases the duct fluid residual time and generates near-wall turbulence [22]. Increasing the number of baffle plates in the longitudinal direction leads to flow

reversal/recirculation, further enhancing turbulence. The Pitch ratio (PR) term defines the distance between the baffle plates. The research was conducted in a circular duct to investigate the impact of changing the PR and α on heat transfer and f . Various PR, ranging from 0.6 to 1.2, and four α (30°, 40°, and 50°) were tested under identical inlet conditions. The Re, estimated using D_h , ranged from 16000 to 28000. The superiority of different configurations was determined by comparing the results of ducts equipped with deflector baffle plates (DBP) to ducts with SBP having the same BR, PR, and Re.

2. Methodology

2.1 Experimental Setup

The experimental setup shown in Figure 1 consists of an axial flow fan, a mixing device, a straightener, a heat exchanger (HX), thermocouple probes, an orifice plate, pressure transducers, and a data acquisition system. The fan sucks atmospheric air from the environment and runs it through the air duct. The air flows through the mixing device and straightener before entering the HX. Temperature probes are installed at the inlet ($T_{a, in}$) and outlet ($T_{a, out}$) portions of the HX as ASHRAE standard recommended [23], and calibrated T-type copper-constantan thermocouples probes are used to measure the air temperature. Orifice plates are operated according to the ISO5801 standard to measure the airflow rate. Pressure ports are also generated, located at 120° angle to the center of the baffle plate, with 3 on the inlet and 3 on the exit side. A VDAS DAQ card, with a differential transducer of 0-1 psi, is used to measure the pressure drop and the LabVIEW program records the data. The water is heated to a constant temperature of 60°C by 8 kW electrical heating elements controlled by a thermostat. The airflow rate is calculated using Eq. (4) and (5), using data from the orifice plate.

Consistency of liquid characteristics (density and temperature) inside the bathtub is ensured using mechanical mixers. A 0.25 hp feed pump, a flow regulating valve, and a flow-measuring device are being used to manage the quantity of hot liquid, which is available continuously at 4 LPM with the help of the flow-measuring device into a header from which it is evenly spread to a heat exchanger tube network. The tubes have been mounted in the HX on baffles that are spaced out at regular intervals. Details of the baffles and the position of the tubes can be found in the following paragraph. RTDs of the PT100 type have been employed to measure the temperature of the hot water-carrying piping at various points in the testing arrangement. A constant LPM of hot water at a set inlet temperature is provided throughout the trial while adjusting the flow rate of air circulation. Before recording data, the system was let to reach a steady state. The

temperatures of the air entering and exiting the HX and the surface temperature of the copper tubing were recorded after the HX had been stabilized, and the repeatability of the experimental outcome was verified thrice and an average standard deviation of 1.46. The root mean square was utilized to evaluate the precision of the immediate measuring device, and Table 1 displays the conditions under which the heat exchangers were tested. Coleman and Steele [24] gave two tables (2 and 3) illustrating the uncertainties involved.

Table 1. Testing conditions used in experiments.

Air-intake temperature	32.5 ± 0.5 °C
Air-intake velocity	7- 10 m/s
Water-intake temperature	60 -65 °C
Mass flow rate of water,	0.06 kg/s

Table 2. Precision with measurements.

Variable	Accurateness
Temperature of air-intake, °C	±0.5
Δp , Pa	±0.1
Temperature of water-intake, °C	±0.5
Flow rate of water, kg/s	±0.006

Table 3. Uncertainties in the experimental data.

Variables	Max skepticism (%)
Re	±3.25
Nu_m	±3.45
v	±5
f	±5.34
Q	±5

2.2 Test Section Details

The part of the system shown in Figure 2 consists of Plexiglas with $kp=0.2$. It has a length of 60 cm, an internal diameter (ID) of 19 cm, and a thickness of 0.5 cm. Running parallel to this Plexiglas is a channel in which DHP Copper tubes, C12200, of $k_r=300$ with ID 8mm and thickness 1mm have been installed. The warm liquid or gas is transported through copper pipes, while the air from the environment is directed through the duct. Two series of thermocouples are employed to determine the temperature of the copper pipes, with each set composed of five thermocouples for each pipe.

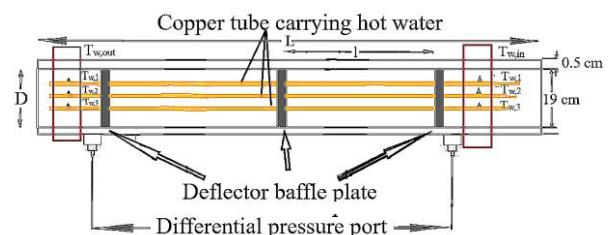


Figure.2. Test section.

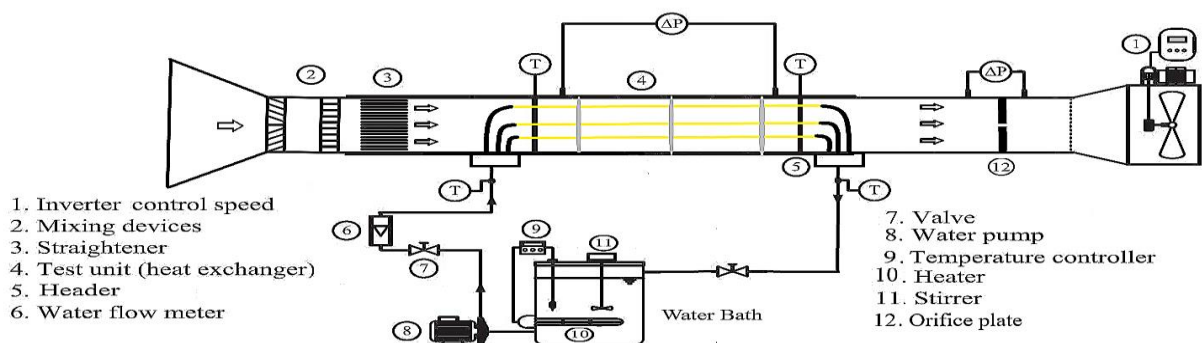


Figure.1 The experimental setup's schematic. [15].

These thermocouples, labeled T_{w1} - T_{w5} , are used to record the temperature of the copper pipe inlets and outlets. To further analyze the air temperatures at the inlet and exit of the test section, $T_{a, in}$, and $T_{a, out}$ thermocouples, are added.

2.3 Baffle Plate with Tube Arrangement

Figure 3(a) and (b) show the novel DBP and SBP, respectively, with one tube at the center and four arranged in a circular array 4cm away from the center of the baffle plate. The dimensions of the rectangular perforation seen in Figure (a) are estimated by equating the BR for DBP and SBP estimated using Equation .2. The novel baffle plate shown in

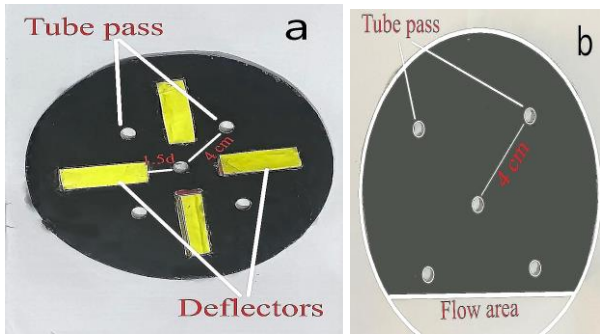


Figure.3(a). DBP five tube configurations, (b). SBP.

Figure 4 (a) with a pictorial view in Figure 4(c) is made of a 5mm Plexiglas sheet cut into circular cross-sections of 19mm diameter using a CNC glass-cutting machine. Later four rectangular holes of (5d x 1.5d) and a center distance of 1.5d are punched in the Baffle plate at an angle of 90 °with each other, which allows air inflow in the test section. Four deflectors of the identical dimension as the rectangular opening (made of 3mm Plexiglas) have been fixed at the preferred inclination angle (α) to the baffle plate, as seen in Figure 4 (b). The inclination of the deflectors thus generates a passage for air, called a flow area of constant height (h). This configuration aids in transitioning the airflow from an axial to a swirling flow. As a result of the deflector, the flow between the baffle plates becomes circular, and the airflow morphs into a smooth swirling pattern as it passes through the tube bundles. When " α " is present, the axial flow intensifies and transforms into a plug flow. The spinning motion increases pressure and enhances a significant portion of the heat transfer between the baffle plates. The distance between the baffle plates dictates the turbulence and circulation within the channel, making the baffle plate's pitch ratio, (PR) important. Values of 0.6, 0.8, 1, and 1.2 were investigated to examine the influence of PR. Consequently,

the rotational air structures bring forth turbulence and foster the formation and movement of vortices within the duct. This leads to continuously washing the tube wall and manipulating the thermal boundary layer. The study encompasses three α angles, namely 30°, 40°, and 50°. This configuration creates an opening that allows air to circulate, effectively functioning as a flow area.

2.4 Design Constraint under Investigation

PR [19, 20] is estimated as

$$PR = \frac{l}{D} \quad (1)$$

BR [25] is estimated as

$$BR = \frac{K}{A} \quad (2)$$

Where, K=cross-sectional area of baffle plate - (4 times the cross-sectional area of the rectangular opening) and, A=cross-sectional area of the baffle plate.

This study assessed the flow of DBP in a round conduit with a constant BR of 0.70 for a longitudinal flow at distinct Re with samples at three different angular inclinations (30°, 40°, and 50°). A further experiment was conducted with a duct without SBP of the same BR at comparable Re ranges. The outcomes of the examination were then examined to determine the impact of PR and α on the TEF of the HX.

2.5 Data Reduction

Cao's [26] technique is employed to assess h_m . These governing parameters are listed below.

$$Re = \frac{\rho v D_h}{\mu} \quad (3)$$

The average bulk temperature of the air-side intake and outlet is utilized to assess the thermal properties of air, such as ρ and μ (viscosity).

$$v = \sqrt{\frac{2\Delta P_0}{\rho}} \quad (4)$$

$$Q_{air} = C_f A_0 \sqrt{\frac{2\Delta P}{\rho}} \quad (5)$$

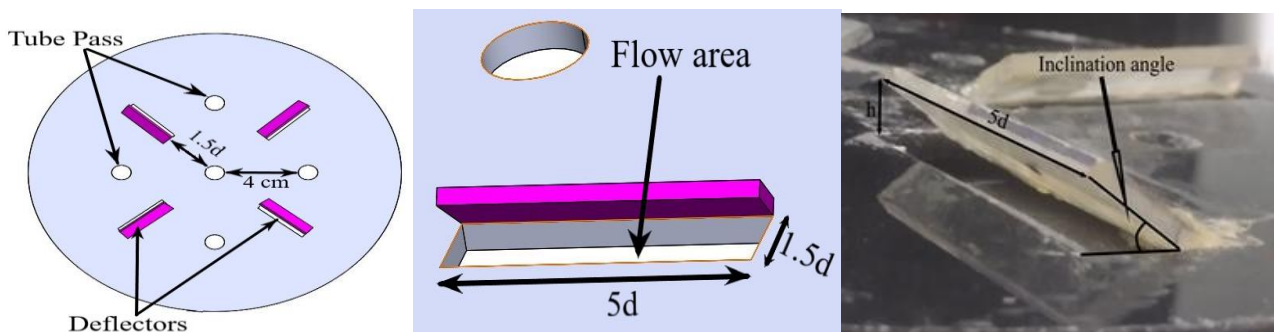


Figure 4 (a). DBP has five tube arrangements, (b).Flow area details, (c) Inclination angle.

$$h_m = \frac{Q}{A_p \Delta t_{lm}} \quad (6)$$

$$Q = C_p \rho v A_c (T_{a,out} - T_{a,in}) \quad (7)$$

The air temperature entering the test section is labeled as $T_{a,in}$, while the temperature of the air as it exits is referred to as $T_{a,out}$, Δt_{lm} is calculated as

$$\Delta t_{lm} = \frac{(t_{w,in} - t_{a,in}) - (t_{w,out} - t_{a,out})}{\ln \left(\frac{t_{w,in} - t_{a,in}}{t_{w,out} - t_{a,out}} \right)} \quad (8)$$

The average copper tube wall is calculated by finding the average inlet temperature ($t_{w,in}$) and the outlet temperature ($t_{w,out}$).

$$t_{w,in} = \left[\frac{\sum_1^5 T_{w,i} A_i}{A_p} \right]_{in}, t_{w,out} = \left[\frac{\sum_1^5 T_{w,i} A_i}{A_p} \right]_{out} \quad (9)$$

For each of the sections specified by subscript i , where i is 1-5, the heat transfer area, A_i , is associated with the location of a thermocouple on the tube carrying hot water in the test section at the inlet and outlet concerning the direction of airflow.

Average Nu , f , and j describe the thermal and flow characteristics.

$$Nu = \frac{h_m D_m}{\lambda} \quad (10)$$

$$j = \frac{Nu}{Re Pr^{1/3}} \quad (11)$$

$$f = \frac{2 \Delta p D}{\rho v^2 L} \quad (12)$$

From Equations 5 and 6

$$h_{c,m} = \frac{C_p \rho v A_c (T_{a,out} - T_{a,in})}{A_p \Delta t_{lm}} \quad (13)$$

Dimensionless factors like (j/j_0) , (f/f_0) , and $[TEF = (j/j_0)/(f/f_0)^{1/3}]$ respectively were used. Using the measured values of f_0 and j_0 of a duct without baffles as benchmarks, compare the corresponding values (f and j) of the duct installed with DBP [15,16].

3. Result and Discussion

3.1 Authentication of the Experimental Outcome

The Nu_m and f obtained from the experiment are compared with correlation Eq. (10) and (12) for precise measurement.

Nu correlations:

a) Dittus and Boelter correlation [27]

$$Nu_s = 0.023 Re^{4/5} Pr^{0.4} \quad \text{For } Re \geq 1 \times 10^4 \quad (14)$$

b) Gnielinski

$$Nu_s = \frac{\left(\frac{f}{8} \right) (Re - 1000) Pr}{\left[1 + 12.7 \left(\frac{f}{8} \right)^{1/2} (Pr^{2/3} - 1) \right]} \quad (15)$$

The correlation is valid for $0.5 \leq Pr \leq 2000$ and $3000 \leq Re \leq 5 \times 10^6$

Friction factor correlation:

a) Colebrook-White correlation [28]:

$$\frac{1}{\sqrt{f}} = 1.8 \log \left(\frac{Re}{6.9} \right) \quad \text{For } 4000 \leq Re \leq 10^8 \quad (16)$$

b) Blasius

$$f = 0.316 Re^{-0.25} \quad \text{for } 3000 \leq Re \leq 5 \times 10^6 \quad (17)$$

The deviation between experimental results and the outcomes obtained using correlation, as shown in Figure 5, confirms the accuracy of the experimental findings. The absolute deviation between these results is indicated in Table 4.

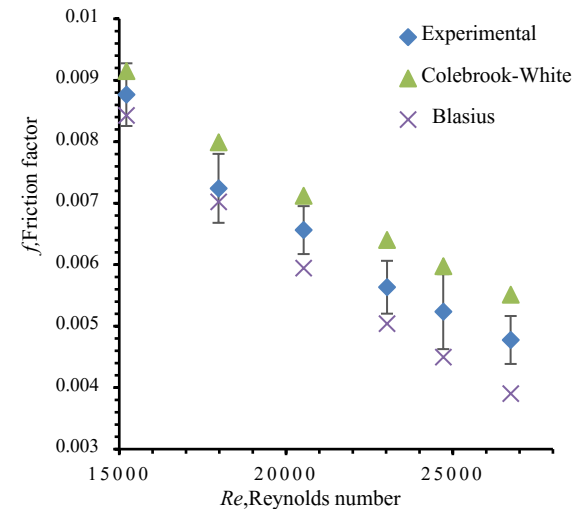
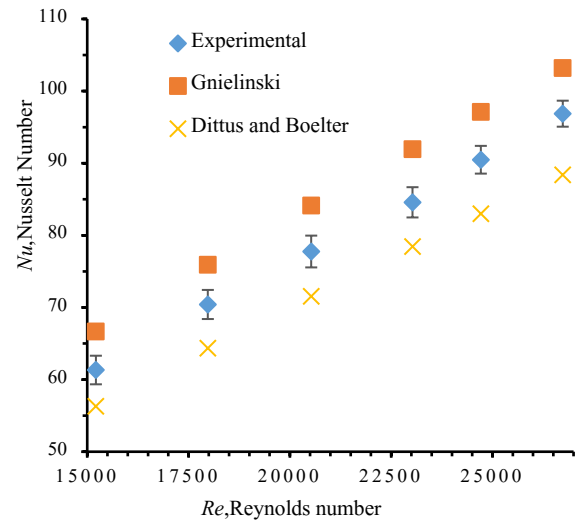


Figure 5. Contrast of Nu and f for duct without baffle plate (Nu_s vs. ;(b) f vs. Re).

Table 4. Average Deviance from Empirical Correlation.

	Nu		f
Correlation used↓	Avg. Deviation i n %	Correlatio n used↓	Avg. deviation i n %)
Dittus and B oelter	-8.180	Colobroo k	+11.066
Gnielinski	+9.054	Blasius	-9.88

3.2 Heat Transfer Augmentation

The presence of a deflector baffle contributes to a significant boost in heat transfer rate over the specified Re range due to the development of powerful reverse flow and the destruction of the thermal boundary layer. Figure 6 shows the fluctuation in relative j/j_0 with Re . The j/j_0 values for DBP rise with a rise in Re to attain a maximum value beyond which it decreases. This fashion in j/j_0 is analogous to all the inclination angles of DBP. DBP with a smaller inclination angle ($\alpha=30^\circ$) shows the highest relative values compared to others α . In turbulent motion, the energy associated with the random fluid motions, known as eddy energy, is transferred throughout the fluid. This random motion creates many small convective cells, allowing heat transfer to occur faster than in a laminar flow because these cells can transport a considerable amount of energy through a large area. Additionally, eddies increase the effective surface area for

near the tube and duct wall. Thus, it is unavoidable that a higher pressure loss will be incurred to increase the heat transfer rate. As revealed in Figure 6, due to the sudden decline in flow passage area for baffles with smaller α , the duct side fluid velocity increases, which results in a jet effect and destruction to the boundary layer formation over the tube and wall, also the fluid revolution washes the tube bundles. The spiral motion produces good mixing, directly leading to improved heat transfer. Moreover, a higher flow velocity enhances the duct-side fluid flushing ability.

As Re further increases, the flow velocity also increases. This higher velocity can cause a reduction in the residence time of the fluid near the heat transfer surface. As a result, there may be insufficient time for effective heat exchange to occur, leading to lower heat transfer rates. Furthermore, the flow may exhibit a more fully developed turbulent profile at higher Re , resulting in a thicker inertial sublayer near the surface, which acts as a thermal resistance, impeding heat transfer. An increase in Re can lead to the forming of flow separation or recirculation zones. These stagnant regions can restrict heat flow and reduce heat transfer efficiency. While it is generally expected that higher Re would correspond to higher heat transfer rates, in current cases, the above factors can lead to a decrease in heat transfer with the rise in Re , and the optimum Re and PR values for efficient heat transfer are shown in Table 5. The study by Wang et al. [29] showed the importance of PR , indicating that downstream vortex flow increases with decreasing the down-wash spacing. However, if the spacing is too small, the interaction between the vortex flows will be strong, causing vortex break-up and decreasing heat transfer enhancement. In contrast, larger spacing's will result in too rapid separation of vortex flow from the boundary layer, consequently leading to high-pressure losses. Thus, it is essential to have an appropriate down-wash baffle plate (PR) spacing to maximize heat transfer. To understand the effect of PR , averaged values of relative j/j_0 shows that max relative j/j_0 is obtained at a lower α value and were plotted against PR for different α values. Figure.8 PR value, which explains Wang's claim regarding the secondary flow, vortex formation, and flow reattachment. As depicted in Figure. 7, fluctuating average (j/j_0) occurs with the PR change. The turbulence intensity between the baffle plates changes with PR ; hence heat transfer rate will fluctuate.

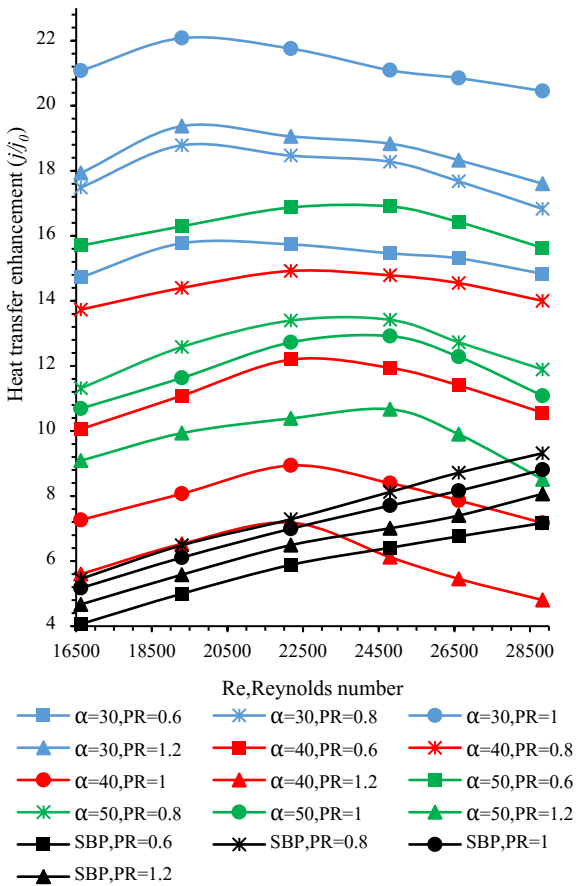


Figure 6. Effect on j/j_0 , with the change in Re .

heat to be conducted from one particle to another, thus accelerating the diffusion process. The circulation of eddies also creates regions of low and high pressure, replenishing the depleted energy necessary for the convection process

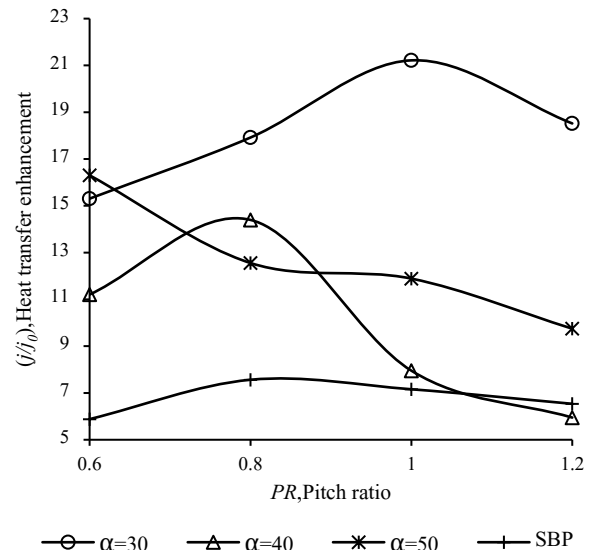


Figure 7. Effect of Averaged (j/j_0) on PR .

Averaged relative j/j_0 is higher for smaller α values and attains a maximum of 21.21 at PR=1 for $\alpha=30^\circ$.

Table 5. Maximum (j/j_0) values.

α	PR	(j/j_0)	Re	% rise compared to SBP
30	1	21.21	18500	62.88
40	0.8	14.39	22100	31.30
50	0.6	16.30	24700	46.25

At a smaller α value, the maximum average (j/j_0) value is noted at a larger PR value and reduces with a surge in α value. An extreme of 21.21 with a percentage rise of 62.88 % in relative Colburn factor is noted when PR=1 and $\alpha=30^\circ$, shown in Table.5, compared to SBP.

3.2 Flow Resistance and TEF

The coefficient of friction was derived from Eq. (12). As shown in Figure 8, the relative friction value (f/f_0) is compared to the Re. In the corresponding range of Re, the Conduit installed with DBP can be expected to present greater flow resistance due to the obstruction in the stream direction. All DBP samples exhibited a similar pattern, exhibiting lower values when the Re was low, gradually increasing with a rise in Re. it is envisioned that the magnitude of the pressure will be in a descending fashion ($\alpha=30^\circ, 40^\circ, 50^\circ$) due to the augmented airflow restriction and vigorous turbulence associated with increased inclination

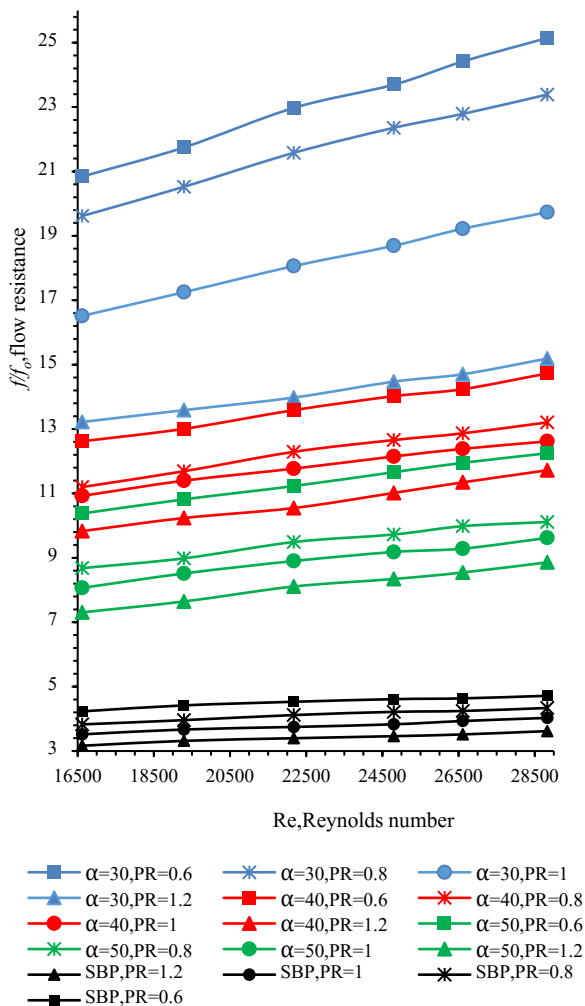


Figure 8. Effect of f/f_0 on Re.

angles resulting in augmented thermal exchange yet intensified friction loss noted when $\alpha=30^\circ$. Consequently, noteworthy pressure drops are revealed as velocities expand, turbulence intensifies, and further connections between the fluid and boundary occur, as seen in Figure 8.

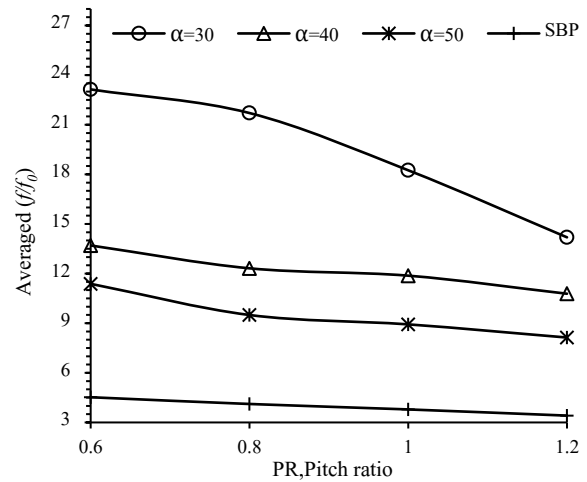


Figure 9. Consequence of α on Average f/f_0 Vs. PR.

Figure 9 demonstrates that the averaged f/f_0 increases as the value of PR and α decreases, reaching a maximum of 23.136 when PR is 0.6, and α is 30° . This can be attributed to a deflector acting as a fluid obstructor, which means that the flow of kinetic energy is lost, resulting in a pressure drop. The minimum value of α provides a powerful swirling flow, increasing the contact between the secondary flow and the duct wall, producing more turbulence and swirl. Due to the vortex formation from several baffles, the flow resistance increases, leading to a significant pressure drop.

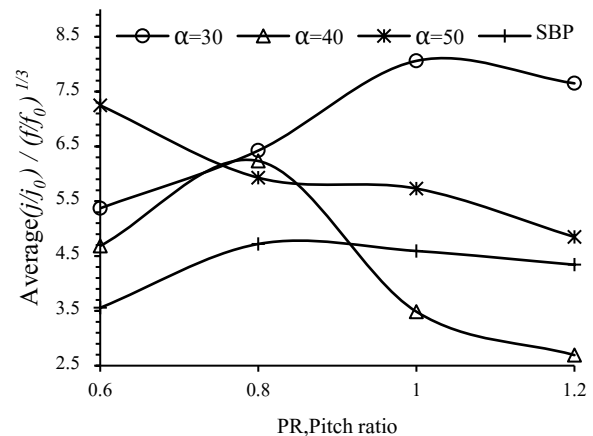


Figure 10. Effect of α on Reynolds average $(j/j_0)/(f/f_0)^{1/3}$ Vs. P_R .

It is observed from Figure 10 that an average increase of 37.43% in TEF value is observed for $\alpha=30^\circ$ when compared to SBP. It can also be concluded that lower α and larger PR values are fruitful for a given Re range. The average rise in TEF compared to SBP is shown in Table 6.

4. Conclusion

Upon comparing DBP samples, it is noted that: The incline angle of the duct showed a considerable impact on the flow velocity; with a tilt of $30^\circ, 40^\circ$, and 50° , Table 6. Averages TEF values.

α	PR	value	% rise compared to SBP
30	1	8.05	41.49
40	0.8	6.23	24.39
50	0.6	7.28	35.30
SBP	0.8	4.71	-----

the velocity was discovered to have increased by 28.07%, 18.57%, and 1.23%, respectively, when compared to the duct with SBP.

The maximum relative j/j_o is at lower Re and lower α for the given Re range. Current HX works best with lower α and higher PR values.

Flow Resistance reduces with an increase in α . The average flow resistance usually reduces with increased PR value but is maximum at PR=0.6.

The average TEF increases with an increase in α and is maximum at $\alpha=30^\circ$ with a value of 8.05 at PR=1

The effect of Pr is negligible due to the working fluid air and the temperature range. Further study needs to be done to explore the user of other liquids such as water, oil, or slurry to explore the possibility of this novel design in shell and tube heat exchangers, exhaust gas heat recovery, gas turbines, and other process industries.

Acknowledgements:

The authors express their gratitude for the facility, help, and support from the Department of Mechanical Engineering, BIT-Mesra, India.

Nomenclature

HX	Heat exchanger
Nu	Nusselt number
TEF	Thermal Performance Factor
R	Thermo-fluid performance
Re	Reynolds number
PR	Pith ratio
f	Friction factor
BR	Blockage ratio
DBP	Deflector baffle plate
SBP	Segmental baffle plate
D	Duct inner diameter
d	Tube outer diameter
v	Average axial velocity (m/s)
D_h	Hydraulic diameter
ΔP	Pressure drop is the test section's (Pa)
Q	Heat transfer rate for air (Watts)
A_p	Heat transfer surface area (m ²)
ΔP_o	Pressure drop in orifice plate in (Pa)
Δt_{lm}	LMTD (Duct and tube wall)
α	Inclination angle
l	Distance between baffle plate(m)
A_c	Flow area (m ²)
D_e	Equivalent diameter (m)
k_p	Thermal conductivity of Plexiglass (W/mK)
k_t	Thermal conductivity of Copper tube (W/mK)
λ	Thermal conductivity of air
ρ	Density of air (kg/m ³)
Pr	Prandtl number of air
h_m	Avg convective heat transfer coefficient (W/m ² .K)
μ	Coefficient of dynamic viscosity (kg/m.s)
Q_{air}	Air discharge

References:

- [1] R.I.Webb, *Principles of Enhanced heat transfer, 1st Ed.* New York: John Wiley-Interscience, 1994.
- [2] A.E. Bergles, "Heat transfer enhancement – the encouragement and accommodation of high heat fluxes," *J. Heat transfer.*, 119, 8–19, 1997, <https://doi.org/10.1115/1.2824105>
- [3] M.Sheikholeslami, M.Gorji-Bandpy, D.D.Ganji, "Review of heat transfer enhancement methods: Focus on passive methods using swirl flow devices," *Renew. Sustain. Energy Rev*, 49, 444–469, 2015, <https://doi.org/10.1016/j.rser.2015.04.113>
- [4] B.N.Prasad, J.S.Saini, "Effect of artificial roughness on heat transfer and friction factor in a solar air heater," *Sol Energy.*, 41,555–60, 1988, [https://doi.org/10.1016/0038-092X\(88\)90058-8](https://doi.org/10.1016/0038-092X(88)90058-8)
- [5] B.N.Prasad, J.S.Saini, "Optimal thermohydraulic performance of artificially roughened solar air heaters," *Solar.*, 47, 91–6, 1991, [https://doi.org/10.1016/0038-092X\(91\)90039-Y](https://doi.org/10.1016/0038-092X(91)90039-Y)
- [6] B.N.Prasad, A.Kumar, K.D.P.Singh, "Optimization of thermo hydraulic performance in three sides artificially roughened solar air heaters," *Sol Energy.*, 111,313–9, 2015, <https://doi.org/10.1016/j.solener.2014.10.030>
- [7] B.Lu, P.X.Jiang, "Experimental and numerical investigation of convection heat transfer in a rectangular channel with angled ribs," *Exp Therm Fluid Sci.*, 30,513–21, 2006, <https://doi.org/10.1016/j.expthermflusci.2005.09.007>
- [8] J.Liu, J.Gao, T.Gao, X.Shi, "Heat transfer characteristics in steam-cooled rectangular channels with two opposite rib-roughened walls," *Appl Therm Eng.*,50,104–11, 2013, <https://doi.org/10.1016/j.applthermaleng.2012.05.003>
- [9] P.Sriromreun, C.Thianpong, P.Promvonge, "Experimental and numerical study on heat transfer enhancement in a channel with Z-shaped baffles," *Int Commun Heat Mass Transf.*, 39,945–52, 2012, <https://doi.org/10.1016/j.icheatmasstransfer.2012.05.016>
- [10] S.Kwankaomeng, P.Promvonge, "Numerical prediction on laminar heat transfer in square duct with 30° angled baffle on one wall," *Int Commun Heat Mass Transf.*, 37, 857–66, 2010, <https://doi.org/10.1016/j.icheatmasstransfer.2010.05.005>
- [11] A.Priyam, P.Chand, "Thermal and thermohydraulic performance of wavy finned absorber solar air heater," *Sol Energy.*, 130,250–9, 2016, <https://doi.org/10.1016/j.solener.2016.02.030>
- [12] V.B.Gawande, A.S.Dhoble, D.B.Zodpe, S.Chamoli, "Experimental and CFD investigation of convection heat transfer in solar air heater with reverse L-shaped ribs," *Sol Energy.*,131,275–95, 2016, <https://doi.org/10.1016/j.solener.2016.02.040>
- [13] S.Eiamsa-Ard, A.Phila, M.Pimsarn, "Heat transfer mechanism and thermal performance of a channel with square-wing perforated transverse baffles installed: effect of square-wing location," *J Therm Anal Calorim.*, 2023, <https://doi.org/10.1007/s10973-022-11937-w>

- [14] M. Sanchouli, S. Payan, A. Payan, S.A.Nada, "Investigation of the enhancing thermal performance of phase change material in a double-tube heat exchanger using grid annular fins," *Case Stud. Therm. Eng.*, 34, 101986, 2022, <https://doi.org/10.1016/j.csite.2022.101986>
- [15] M.A.Rahman, S.K.Dhiman, "Performance evaluation of turbulent circular heat exchanger with a novel flow deflector-type baffle plate," *J Eng Res.*, 100105, 2023, <https://doi.org/10.1016/j.jer.2023.100105>
- [16] M. A. Rahman, S.K.Dhiman, "Investigations of the turbulent thermo-fluid performance in a circular heat exchanger with a novel flow deflector-type baffle plate," *Bull. Pol. Acad. Sci.: Tech.*, 2023, doi: 10.24425/bpasts.2023.145939
- [17] T.Alam, M.Kim, "Numerical study on thermal hydraulic performance improvement in solar air heater duct with semi ellipse shaped obstacles," *Energy.*, 112,588–98, 2016, <http://dx.doi.org/10.1016/j.energy.2016.06.105>
- [18] J. Guo, A.W. Fan, X.Y. Zhang, W. Liu, "A numerical study on heat transfer and friction factor characteristics of laminar flow in a circular tube fitted with center-cleared twisted tape," *Int. J. Therm Sci.*, 50, 1263–1270, 2011, <https://doi.org/10.1016/j.ijthermalsci.2011.02.010>
- [19] C.Thianpong, P.Eiamsa-ard, K.Wongcharee, S.Eiamsa-ard, "Compound heat transfer enhancement of a dimpled tube with a twisted tape swirl generator," *Int Commun Heat Mass Transf.*,36,698–704, 2009,<https://doi.org/10.1016/j.icheatmasstransfer.2009.03.026>
- [20] E.Esmaeilzadeh, H.Almohammadi, A.Nokhosteen, A.Motezaker, A.N.Omrani, "Study on heat transfer and friction factor characteristics of Al₂O₃ water through circular tube with twisted tape inserts with different thicknesses," *Int J Therm Sci.*, 82, 72–83, 2014, <https://doi.org/10.1016/j.ijthermalsci.2014.03.005>
- [21] M.M.K.Bhuiya, A.S.M.Sayem, M.Islam, M.S.U.Chowdhury, M.Shahabuddin, "Performance assessment in a heat exchanger tube fitted with double counter twisted tape inserts," *Int Commun Heat Mass Transf.*,50,25–33,2014, <https://doi.org/10.1016/j.icheatmasstransfer.2013.11.005>
- [22] A.Durmus, M.Esen, "Investigation of heat transfer and pressure drop in a concentric heat exchanger with snail entrance," *Appl Therm Eng.*, 22(3), 321–32, 2002, [https://doi.org/10.1016/S1359-4311\(01\)00078-3](https://doi.org/10.1016/S1359-4311(01)00078-3)
- [23] ASHRAE Handbook-Fundamental, *Principles of Heating, Ventilation and Air-conditioning Engineers*, 8th Ed. Atlanta: American Society of Heating, Refrigerating and Air-Conditioning Engineers, Inc., chap. 13, 14–15, 1993.
- [24] H.W.Coleman,W.G. Steele, *Experimentation, validation, and uncertainty analysis for engineers*, 4th Ed. New York: John Wiley & Sons, 2018.
- [25] J.D.Holmes, *Wind Loading of Structures*, 2nd Ed. New York: Taylor & Francis, 168-169, 2007.
- [26] Y.Z.Cao, *Experimental Heat Transfer*, 1st Ed. Beijing: National Defense Industry Press, 120-125, 1998.
- [27] F.W.Dittus, L.M.K.Boelter,*Heat Transfer in Automobile Radiators of the Tubular Type*, Berkley: University of California Press, 2, 443, 1930.
- [28] F.W.White, *Fluid mechanics*, 3rd Ed. New York: McGraw-Hill, 2003.
- [29] J.L.Wang, Z.S.Zhang, X.Zeng, "Effect of longitudinal vortices on the turbulent structure in near-wall region," *Acta Mechanica Sinica.*, 26(5), 1994, 625e629 (in Chinese).